Title: Gene delivery in the cornea: *in vitro* and *ex vivo* evaluation of solid lipid nanoparticle-based vectors

Short running title: Non-viral vectors for corneal transfection

Authors: Mónica Vicente-Pascual[1], Andrea Albano[1,2], María Angeles Solinís[1], Loredana Serpe[2], Alicia Rodríguez-Gascón[1], Federica Foglietta[2], Elisabetta Muntoni[2], Josune Torrecilla[1], Ana del Pozo-Rodríguez*[1], Luigi Battaglia[2]

1. Pharmacokinetic, Nanotechnology and Gene Therapy Group (PharmaNanoGene), Faculty of Pharmacy, Centro de investigación Lascaray ikergunea, University of the Basque Country UPV/EHU, Paseo de la Universidad 7, Vitoria-Gasteiz, Spain.

2. Università degli Studi di Torino, Dipartimento di Scienza e Tecnologia del Farmaco, via Pietro Giuria 9, Turin, Italy.

* corresponding autor: Ana del Pozo Rodríguez (e-mail: ana.delpozo@ehu.eus; phone: +34 945014498)

Financial disclosure: This work was supported by the Spanish Ministerio de Economía y Competitividad (SAF2014-53092-R), by FEDER funds from the EU, by the UPV/EHU (PPG17/65, GIU17/032 and J Torrecilla's research grant), and by Italian Ministero dell'Università e Ricerca (MIUR – Ricerca Locale 2016-2017).

Ethical disclosure: The authors state that they have obtained appropriate institutional review board approval or have followed the principles outlined in the Declaration of Helsinki for all animal experimental investigations.

Author Contributions:

Mónica Vicente-Pascual contributed to the acquisition, analysis and interpretation of experimental results, drafted the work and approved the final version.

Andrea Albano contributed to the acquisition, analysis and interpretation of experimental results, critically revised the work and approved the final version.

Mª Angeles Solinís contributed to work design, and to the analysis and interpretation of experimental results, critically revised the work and approved the final version.

Loredana Serpe contributed to the acquisition, analysis and interpretation of experimental results, critically revised the work and approved the final version.

Alicia Rodríguez-Gascón contributed to work design, and to the analysis and interpretation of experimental results, critically revised the work and approved the final version.

Federica Foglietta contributed to the acquisition, analysis and interpretation of experimental results, critically revised the work and approved the final version.

Elisabetta Muntoni contributed to the acquisition, analysis and interpretation of experimental results, critically revised the work and approved the final version.

Josune Torrecilla contributed to the acquisition, analysis and interpretation of experimental results, critically revised the work and approved the final version.

Ana del Pozo-Rodríguez contributed to work design, and to the analysis and interpretation of experimental results, critically revised the work and approved the final version.

Luigi Battaglia contributed to work design, and to the analysis and interpretation of experimental results, critically revised the work and approved the final version.

Word count: 7,472 (without references)
Figure number: 10
Table number: 5

Abstract: Background: Inflammation is an underlying process of ocular surface diseases resulting in visual loss. Gene supplementation with the plasmid that encodes for Interleukin-10 (p-IL10) will provide the sustained *de novo* synthesis of the cytokine in corneal cells, and a long-term anti-inflammatory effect. In this work, p-IL10 delivery systems based on SLNs were developed, for the topical management of corneal inflammatory related diseases. **Results:** After *in vitro* characterization, the vectors were able to transfect the epithelium, the stroma, and the endothelium in rabbit corneal explants. **Conclusion:** SLN-based vectors are promising gene delivery systems, useful for inflammation related corneal diseases. Depending on the SLN composition and the surface coating, the biodistribution within the cell layers of the cornea may be modulated.

Background: Inflammation is a process that underlies sight-threatening ocular surface diseases, and gene supplementation with the plasmid that encodes for interleukin-10 (p-IL10) will allow the sustained *de novo* synthesis of the cytokine to occur in corneal cells, and provide a long-term anti-inflammatory effect. This work describes the development of solid lipid nanoparticle (SLN) systems for the delivery of p-IL10 to transfect the cornea. **Results:** *In vitro*, vectors showed suitable features as non-viral vectors (size, zeta potential, DNA binding, protection and release), and they were able to enter and transfect human corneal epithelial cells. *Ex vivo*, the vectors were found to transfect the epithelium, the stroma and the endothelium in rabbit corneal explants. Distribution of gene expression within the cell layers of the cornea depended on the composition of the four vectors evaluated. **Conclusion:** SLN-based vectors are promising gene delivery systems for corneal diseases, including inflammation.

Graphical abstract:

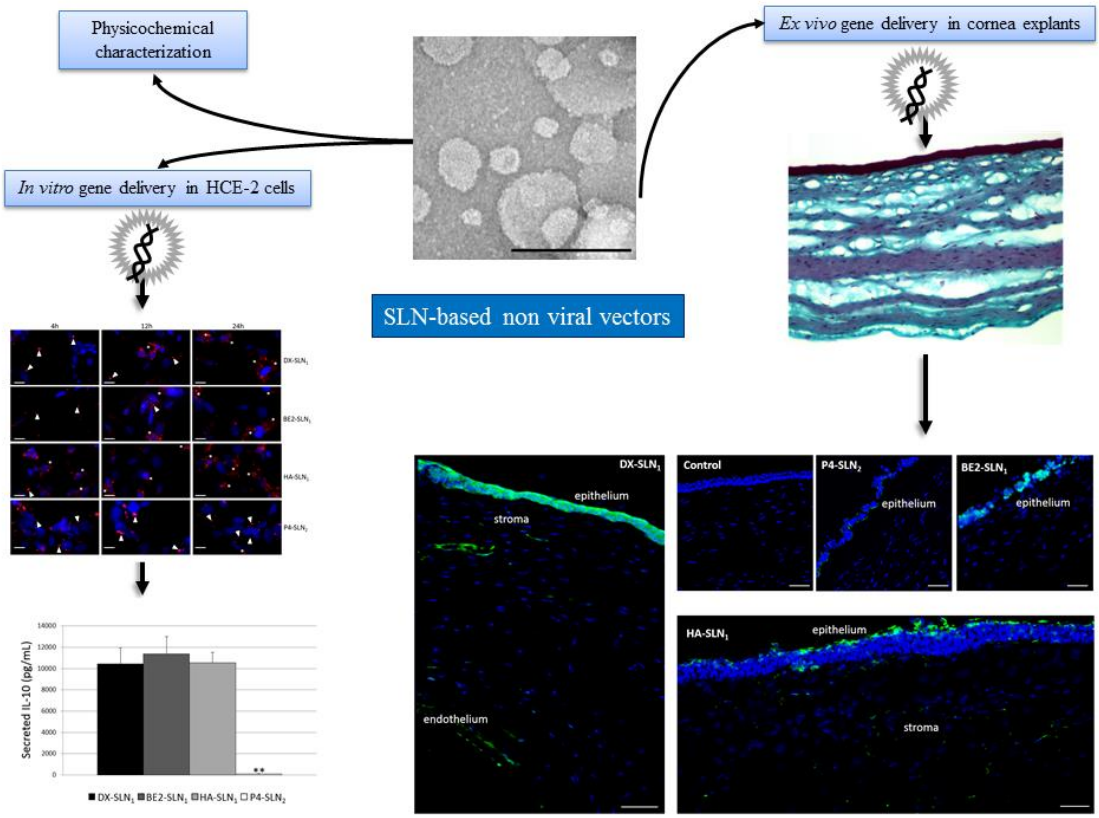

Keywords: solid lipid nanoparticles; non-viral vectors; corneal transfection; corneal inflammation; interleukin-10 gene; gene delivery; cornea explant; gene supplementation; in vitro; ex vivo

1. Introduction

Inflammation is the underlying process in severe ocular surface diseases, such as dry eye syndrome, allergic diseases and contact lens-related injuries as well as bacterial and viral infections [1]. The chronic inflammation associated with these conditions alters the corneal epithelial barrier [2], and results in vision loss and an impairment in life quality. The conventional therapy against ocular inflammation is the systemic administration or topical instillation of corticosteroids [3]. However, cataracts and increased intraocular pressure are adverse effects that are frequently caused by the long-term use of corticosteroids. Therefore, the development of new therapeutic strategies for the treatment of corneal inflammation becomes necessary.

One possible approach is the administration of interleukin-10 (IL-10). This soluble and multifunctional cytokine, which is produced by several types of cells, displays both anti-inflammatory and immunosuppressive effects [4]. Several studies have confirmed the essential role that IL-10 plays in the regulation of bowel inflammation, chronic infections and neuroimmune diseases [5, 6], in the avoidance of allograft rejections [7, 8], and in the immune response associated to ocular surface pathologies. Specifically in terms of ocular diseases, treatment with IL-10 in animal models has proven to be successful in promoting corneal transplant survival [9], and modulating herpes simplex virus (HSV)–induced stromal keratitis (HSK) [10], which is a significant infectious cause of blindness in developed nations. The blinding illness in ocular HSV infections is not the result of viral replication, but rather of the subsequent host immunologic response to the virus. It is here that the properties of IL-10 have been found to play a protective role in mice HSK models. However, the low bioavailability of this protein after topical administration, which is caused by the corneal barrier, and its short half-life, hamper the anti-inflammatory effect, even after frequent topical administration at high doses. Gene supplementation, in which the plasmids that encode for IL-10 (p-IL10) are administered in the cornea, is an alternative that may overcome these drawbacks. An important benefit of this therapy is the sustained synthesis of the protein *de novo* in corneal cells, which provides a long-term anti-inflammatory effect.

The well-known need for suitable delivery systems that can facilitate successful gene therapy must be considered. Ideally, a system for corneal gene delivery must meet certain requirements: manufacture at high concentration and purity using simple and

reproducible procedures, corneal cell targeting to provide high therapeutic gene levels in a tissue-selective manner, and a lack of local toxicity, immunological reaction and injury to the extracellular matrix and surrounding tissues [11]. In this sense, cationic solid lipid nanoparticles (SLNs) present several advantages for corneal gene therapy. SLNs consist of a solid lipid core surrounded by a layer of surfactants in an aqueous dispersion and are usually composed of well-tolerated physiological lipids, that have been approved for pharmaceutical preparations for human use [12]. Furthermore, a variety of production methods, which have been successfully implemented in the pharmaceutical and cosmetic industries have been developed to manufacture SLNs and have furnished stable delivery systems that can undergo long-term storage [13]. Regarding delivery to the cornea, their nanometre-range dimensions and lipophilic properties mean that SLNs can enhance corneal penetration and the cellular uptake of active molecules, extend ocular retention time and provide a controlled release profile, improving ocular bioavailability [14-17]. Concerning their use as gene delivery systems, SLNs have been documented to be one of the most effective lipid-based non-viral vectors, both *in vitro* and *in vivo* [18-21]. Moreover, these nanoparticles may be functionalized with a number of ligands to overcome barriers for gene transfer, such as, interaction with targeted cells, cellular uptake, appropriate intracellular distribution and entry to the nucleus. Chitosan, dextran and hyaluronic acid [22-24], which have received recognition for their biocompatibility, biodegradation and mucoadhesive properties, are such ligands and are commonly used in the design of ocular drug delivery systems [25, 26].

The aim of this study is the development of p-IL10 delivery systems for transfection in the cornea, which may be useful for the topical therapeutic management of corneal inflammation-related diseases. After the physicochemical characterization of the SLN-based vectors, their efficacy and intracellular behaviour in human corneal epithelial cells was studied, and their capacity to transfect corneal tissues was evaluated *ex vivo* in corneas that had been explanted from rabbits.

2. Materials and methods

2.1. Materials

DOTAP (1,2-Dioleoyl-3- trimethylammonium-propane chloride salt) was obtained from Avanti Polar-lipids Inc. (AL, USA), Tween 80 and dichloromethane from Panreac

(Madrid, Spain), sodium behenate from Nu-Chek Prep (Eleysian, AL, USA) and Precirol® ATO5 was generously provided by Gattefossé (Madrid, Spain). Protamine sulfate salt Grade X (P), dextran (Mw of 3.26 KDa) (DX), ammonium chloride, glycol chitosan (CH), partially hydrolyzed polyvinyl alcohol 9000-10000 Da Mw (PVA9000) and Nile Red were acquired from Sigma-Aldrich (Madrid, Spain). Hyaluronic acid (Mw of 100 KDa) (HA) was purchased from Lifecore Biomedical and Bemiparin was a kind gift from Rovi® (Spain). The plasmid pcDNA3-EGFP (6.1 kb), that encodes the green fluorescent protein (GFP), was kindly provided by the laboratory of Professor B.H.F. Weber (University of Regensburg, Germany) and pUNO1-hIL10 (3.7 kb), which encodes human IL-10, was provided by InvivoGen. The promoter in this second plasmid (hEF1/HTLV) comprises the Elongation Factor-1α (EF-1α) core promoter coupled to the R segment and the U5 sequence (R-U5') of the Human T-Cell Leukemia Virus (HTLV) Type 1. According to the manufacturer, this combination increases the steady state transcription and significantly increases translation efficiency.

Deoxyribonuclease I (DNase I) and sodium dodecyl sulphate (SDS) were obtained from Sigma-Aldrich (Madrid, Spain), GelRed™ from Biotium (California, USA) and the materials used in electrophoresis on agarose gel were purchased from Bio-Rad (Madrid, Spain).

Cell culture reagents, including Dulbecco´s Modified Eagle´s Medium/Nutrient Mixture F-12 with GlutaMAX™ (DMEM/F-12 with GlutaMAX™), fetal bovine serum (FBS) and penicillin-streptomicin, were acquired from Life Technologies (ThermoFisher Scientific, Madrid, Spain). Human insulin solution was obtained from Sigma-Aldrich, EGF from Myltenyi Biotec and Trypsin-EDTA from Lonza.

Triton X-100 and DNA from salmon sperm were provided by Sigma-Aldrich (Madrid, Spain), Reporter Lysis Buffer (RLB) by Promega Biotech Ibérica (Madrid, Spain), and DAPI-Fluoromount-G by Southern Biotech (Birmingham, USA). Paraformaldehyde (PFA) was obtained from Panreac, while PBS and HEPES buffer were purchased from Gibco (ThermoFisher Scientific, Madrid, Spain). Transfectin® Lipid-Reagent was acquired from Bio-Rad, while ELISA for IL-10 with the DuoSet Ancillary reagent kit was purchased from R&D Systems.

The tissue-Tek® O.C.T™ compound was obtained from Sakura Finetek Europe (Leiden, The Netherlands). Other chemicals, unless specified, were reagent grade from Sigma Aldrich (Madrid, Spain) and Panreac (Barcelona, Spain).

2.2. Preparation of SLNs and vectors

SLNs were prepared using two different techniques: solvent evaporation/emulsification (SLN_1), which has previously been described [21], and coacervation (SLN_2), which was partially modified from [27] and [28]; the precipitation of SLN_2 was obtained using 5 M ammonium chloride and 1 M hydrochloric acid, instead of 1 M sodium phosphate and 1 M hydrochloric acid.

SLN_1 were made up of a core of the solid lipid Precirol® ATO5 and a cationic lipidic surface based on DOTAP and the surfactant Tween 80. In order to prepare SLN_1-based vectors, the plasmid (pcDNA3-EGFP or pUNO1-hIL10) was first mixed with an aqueous solution of protamine (P) and then with an aqueous solution of either the polysaccharide dextran (DX), bemiparin (BE) or hyaluronic acid (HA). The complexes obtained were added to the SLN_1 suspension, and the electrostatic interactions led to the binding of the complex by the SLNs, and to the formation of the final vector. The weight ratios of the components are summarized in Table 1.

SLN_2 were composed of behenic acid as the lipid matrix, were coated with PVA9000, as the suspending agent, and used CH as the cationizing agent. In order to prepare SLN_2-based vectors, the plasmid was first complexed with P, and then with the SLN_2. Vectors with different P:DNA:SLN_2 ratios were prepared (Table 1).

Table 1. Weight ratios of the vectors prepared and evaluated.

Name of the vector	Polysaccharide	Weight ratio
DX-SLN_1	DX	DX:P:DNA:SLN_1 1:2:1:5
BE2-SLN_1	BE	BE:P:DNA:SLN_1 0.1:2:1:5
BE3-SLN_1	BE	BE:P:DNA:SLN_1 0.1:3:1:5
HA-SLN_1	HA	HA:P:DNA:SLN_1 0.5:2:1:2
DNA-SLN_2	-	P:DNA:SLN_2 0:1:20
P2-SLN_2	-	P:DNA:SLN_2 2:1:5
P4-SLN_2	-	P:DNA:SLN_2 4:1:10

2.3. Size and zeta potential measurements

A Zetasizer Nano series-Nano ZS (Malvern Instruments, Worcestershire, UK) was used to measure size, polydispersity index and superficial charge of SLNs and the final vectors. The samples were diluted in Milli-Q™ water (EDM Millipore, Billerica, MA) for the particle size and zeta potential measurements, which were carried out using photon correlation spectroscopy (PCS) and Laser Doppler Velocimetry (LDV), respectively.

2.4. Transmission electronic microscopy (TEM) images

TEM images of the SLN_1 and SLN_1-based vectors were already present in the literature [21]. Visualization of SLN_2 and the SLN_2-based vectors was performed using electron microscopy negative staining. For that purpose, 10 µl of the sample was adhered onto glow discharged carbon coated grids for 60 s. After removing the remaining liquid, via blotting on filter paper, the staining was carried out with 2% uranyl acetate for 60 s. Samples were visualized using a Philips EM208S TEM and digital images were acquired on an Olympus SIS purple digital camera. Technical and human support for TEM was provided by the General Service (SGIker) of Analytical Microscopy and High Resolution in Biomedicine at the University of the Basque Country UPV/EHU.

2.5. Agarose gel electrophoresis assay

With the aim of studying the DNA binding efficiency of the vectors, the protection from DNase I digestion and the SDS-induced release of DNA, 0.7% agarose gel electrophoresis containing Gel Red™ was used and analysed using an Uvitec Uvidoc D-55-LCD-20M Auto transilluminator, as previously described [22]. The capacity of the vectors to bind electrostatically the DNA was evaluated by adding the complexes at a final concentration of 0.03 µg DNA/µl diluted in MilliQ™ water in the gel. For DNAse I protection, the same concentration was exposed to 1 U DNase I/2.5 µg DNA and then incubated at 37ºC for 30 min. A SDS solution (4%) was mixed with the samples, to a final concentration of 1%, to release DNA from the SLNs. The pcDNA3-EGFP and pUNO1-hIL10 plasmids were added, untreated, as controls, as well as the 1 kb DNA ladder from NIPPON Genetics Europe (Dueren, Germany).

2.6. In vitro studies

The human corneal epithelium (HCE-2) cell line was used for *in vitro* assays. HCE-2 cells were maintained in medium, which was composed of DMEM/F-12 with GlutaMAX™, fetal bovine serum (15%), insulin (4 mg/mL), EGF (10 ng/ml) and penicillin-streptomycin (1%), incubated at 37ºC with 5% CO_2 and subcultured every 7 days.

2.6.1. In vitro transfection

Cells were seeded on 24-well plates at a density of 150,000 cells using 1 ml of medium per well, and then allowed to adhere for 24 hours. Seventy five µl of each vector (2.5 µg DNA) was then added to each well, containing 0.5 ml of medium, and the plates were incubated for 4 hours at 37ºC in 5% CO_2. Thereafter, vectors were removed, cells were refreshed with 1 ml of complete medium, and the cell culture was allowed to grow for 72 hours. Naked plasmids and the complexes without SLNs were also tested at the same dose of DNA. Transfection efficacy obtained with the vectors was compared to that obtained with the commercial transfectant TransFectin® Lipid-Reagent (Bio-Rad, Madrid, Spain), which was used according to the manufacturer's protocol.

2.6.2. Quantification of GFP and cell viability

A fluorometric assay was carried out to quantify intracellular GFP 72 hours after treatment. Briefly, cells were washed with 300 µl of PBS, 400 µl of Reporter Lysis Buffer 1x was then added, and the plate was frozen to complete the lysis of the cell culture. After thawing, each well was scrapped and the lysate was centrifuged at 12,000 g for 2 min at 4ºC. In order to measure the amount of GFP contained in 100 µl of the supernatant at 525 nm, a Glomax Multi Detection System (Promega) was employed, and GFP amount was expressed as Relative Fluorescent Units (RFU). The mean value of the auto-fluorescence detected in the non-treated cells was subtracted from the fluorescence measured in each well, and it was expressed as Relative Fluorescent Units (RFU).

The percentage of transfected cells was measured using a FACSCalibur flow cytometer (Becton Dickinson Bioscienses, San Jose, USA). For this purpose, cells were washed with 0.5 ml of PBS 72 hours after transfection and then detached using 0.5 ml of trypsin-EDTA and, after incubation for 10 min, centrifuged at 1,000 rpm for 5 min. The

supernatant was discarded and cells were resuspended in 0.5 ml of PBS. Ten thousand events were collected for each sample. Transfection efficacy was measured at 525 nm (FL1), and cell viability at 650 nm (FL3). Propidium iodide was employed for dead cell exclusion [23].

2.6.3. Quantification of IL-10

In order to measure the levels of IL-10 expressed by the cells 72 hours after addition of the complexes, an Enzyme-linked Immunosorbent Assay (ELISA) kit was carried out. Secreted and intracellular IL-10 was quantified. In order to quantify intracellular IL-10, cells were detached from the wells and lysed, as described in section 2.7 for intracellular GFP quantification. For secreted IL-10, the medium of each well was retired and centrifuged. One hundred µl of each sample was added to a 96-well plate that was covered with the corresponding capture antibody, and the assay was then performed according to the manufacturer´s instructions.

2.6.4. Cellular uptake of the vectors

In order to study the entrance of the complexes into HCE-2 cells, SLNs were labelled with the fluorescent dye Nile Red (λ=590 nm), and the vectors were prepared as described in section 2.2. Vectors were added to each well, and after 2 hours of incubation at 37ºC, the culture medium was retired and cells washed with PBS before being deteached from the wells, as described in section 2.7 for the percentage of GFP transfected cells. Vector entry into the cells was analysed using a FACSCalibur flow cytometer at 650 nm (FL3).

2.6.5. Intracellular disposition of the vectors

Cells were seeded and incubated at 37ºC, 5% CO_2 for 24 hours in Millicell EZ slides (Millipore) at a density of 150,000 cells and 1 ml per well, and they were then treated with vectors containing the plasmid, which was labelled with ethidium monoazide (EMA). After 4, 12 and 24 hours, the slides were washed with PBS and fixed with PFA 4%. DAPI-fluoromount-G™ (Southern Biotech) was used as the mounting fluid, to label the nuclei. The slides were then studied using an inverted fluorescence microscopy (Nikon TMS).

2.7. Ex vivo studies

Ex vivo studies were performed on rabbit corneas. Eyes were enucleated, within 2 hours after animal death, from 12 week albino rabbits killed in a slaughterhouse for food purposes. Corneas were excised and kept in sterile Steinhardt medium [29], according to a protocol currently used for human cornea trans-plantation. A scleral ring of nearly 4 mm was maintained around the explanted corneas. The internalization of Nile Red-labelled vectors and the transfection efficacy, after treating the corneas with vectors bearing pcDNA3-EGFP, were studied using a previously-documented corneal holder [30]; it is a Plexiglas and glass structure, with donor and receiving compartments (0.65 mL volume). The cornea was placed in the orifice (0.50 cm^2) that divides the two compartments. To minimize the corneal irritation the o-ring holds only the scleral ring around the corneal circumference. Two hundred µl of SLNs under study were diluted to 600 µl with PBS, vortexed for 5 seconds, sonicated for 30 seconds, and then introduced into the donor compartment of the corneal chamber (epithelial side), while the receiving chamber was filled with PBS. In this preliminary study the effect of tear washing was not considered, being the chamber a static system. Thus, the administered volume was constrained by chamber size and cannot resemble the real volume of tear flow. However, it was considered that an eye drop has a volume of nearly 25-56 µL, in front of a tear flow of about 1 µL/min, and the dilution of SLNs in PBS before administration was designed in order to resemble the ratio between administered nanosuspension and tear volume during the 2 hours experiment.

2.7.1. Cell internalization of the vectors

The corneas were kept at 37°C in the chamber for 2 hours, then removed, rinsed with normal saline buffer and observed using fluorescence microscopy on a DMI4000B fluorescence microscope (Leica). The corneas were subsequently still kept in vials with Steinhardt medium at 37°C for 24 hours, prior to further fluorescence microscopy observation. The staining of cell nuclei was performed by incubating the corneas in 1 µM DAPI in PBS for 30 minutes endothelial side up, prior to observation. Images were acquired and merged using the Leica Application Suite V3 software.

2.7.2. *Transfection studies*

The corneas were kept at 37°C in the chamber for 2 hours, then removed from the chamber, rinsed with normal saline and kept in Steinhardt medium at 37°C for 48 hours, allowing GFP protein expression to occur. After incubation, the corneas were fixed with

4% PFA for 30 min and then transferred into a scintillation vial containing 3 mL of PBS 1x. After 5 min, the PBS was replaced with 3 ml of a 30 % sucrose in PBS 1x solution and the sample was incubated overnight at 4°C. After the incubation period, the volume was replaced with 3 mL of Tissue-Tek OCT (Optimum cutting temperature formulation). The cornea was then quick-frozen in liquid nitrogen, and later sectioned (14 µm) on a cryostat (Cryocut 3000, Leica).

GFP detection was performed by immunofluorescence. Sections were fixed with 4% paraformaldehyde for 10 min at room temperature. Next, they were washed in PBS, blocked and permeabilized in PBS 0.1 M, 0.1% Triton X-100 and 2% normal goat serum for 1 hour at room temperature. Subsequently, samples were incubated in primary antibody (polyclonal anti-GFP, IgG fraction) for 2 hours at room temperature, then washed again in PBS, and incubated in secondary antibody (Alexa Fluor 488 goat anti-rabbit IgG). Lastly, sections were washed in PBS and mounted with Fluoromount G. The fluorescence in each sample was analysed using inverted fluorescence microscopy (Nikon TMS).

Sections of the cornea were also analysed using Masson´s trichrome staining technique. All samples were histologically evaluated and examined with an optical microscope (Olympus BX50).

2.8. Statistical analysis

Statistical analysis was performed using IBM® SPSS® Statistics 23 (IBM). The normal distribution of the samples was assessed using the Shapiro-Wilk test, and homogeneity of variance, using the Levene test. Comparisons were performed using either an ANOVA or Student's *t* test. Differences were considered statistically significant at $p<0.05$. Results are expressed as mean±SD.

3. Results

3.1. Size, polydispersity index and zeta potential

Table 2 summarizes the particle size, polydispersity index (PDI) and zeta potential of plain SLNs. As can be seen, SLN_1 had a slightly smaller size than SLN_2 (257 vs 341 nm), while the PDIs were similar and under 0.35 in both cases. Zeta potential was positive, but lower for SLN_2 (+21 vs +42 mV).

Table 2. Physicochemical characterization of SLN_1 and SLN_2. PDI (Polydispersity index). (n=3; data are expressed as mean ± standard deviation).

SLNs	Size (nm)	PDI	Zeta potential (mV)
SLN_1	257.7 ± 6.3	0.32 ± 0.04	+41.8 ± 1.2
SLN_2	341.0 ± 0.9*	0.33 ± 0.00	+21.0 ± 0.8*

**p<0.05 with respect to SLN_1.*

The size of the SLN_1-based vectors bearing the plasmid pcDNA3-EGFP (Table 3) ranged from 143.2 (BE3-SLN_1) to 218.9 nm (HA-SLN_1), while they displayed PDI values that were always lower than 0.35. The surface charge varied from +28.1, in the case of HA-SLN_1, to +39 mV.

Table 3. Physicochemical characterization of SLN_1-based vectors bearing the plasmid pcDNA3-EGFP. PDI (Polydispersity index). (n=3; data are expressed as mean ± standard deviation).

Vectors with pcDNA3-EGFP	Size (nm)	PDI	Zeta potential (mV)
DX-SLN_1	199.8 ± 0.4	0.26 ± 0.01	+38.4 ± 1.6
BE2-SLN_1	198.2 ± 1.6	0.29 ± 0.04	+38.9 ± 2.6
BE3-SLN_1	143.2 ± 7.2*	0.31 ± 0.05	+38.6 ± 1.1
HA-SLN_1	218.9 ± 1.2*	0.32 ± 0.04	+28.1 ± 1.6*

**p<0.05 with respect to the other formulations.*

Regarding SLN_2-based vectors (Table 4), three formulations were characterized. P4-SLN_2 was the smallest in term of size (278 nm) and its zeta potential was the highest (+26 mV). The vector that was prepared without protamine (DNA-SLN_2) was slightly bigger (325 nm; $p<0.05$) and its surface charge was lower (+7.5 mV; $p<0.05$). By contrast, the formulation P2-SLN_2 was the largest (434 nm; $p<0.05$) and its surface charge was the lowest ($p<0.05$), at +4.2 mV. All PDI measurements were under 0.3.

Table 4. Physicochemical characterization of SLN_2-based vectors bearing the plasmid pcDNA3-EGFP. PDI (Polydispersity index). (n=3; data are expressed as mean ± standard deviation).

Vectors with pcDNA3-EGFP	Size (nm)	PDI	Zeta potential (mV)
DNA-SLN_2	325.7 ± 1.2*	0.24 ± 0.01	+7.5 ± 0.2*
P2-SLN_2	434.2 ± 25.4*	0.30 ± 0.02	+4.2 ± 0.2*
P4-SLN_2	278.0 ± 5.7*	0.29 ± 0.01	+26.2 ± 1.3*

**p<0.05 with respect to the other formulations.*

No changes ($p>0.05$) in particle size, PDI or zeta potential were observed (data not shown) when SLNs were labelled with Nile Red

3.2. TEM images

TEM photographs of the SLN_2 (Figure 1A) and P4-SLN_2 vectors (Figure 1B) show the spherical shape of the nanoparticles, as well as of the final vectors.

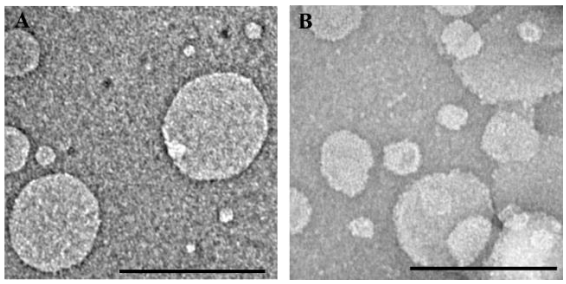

Fig. 1. TEM photographs of (A) SLN_2 and (B) P4-SLN_2 vectors. Scale bar: 200 nm.

3.3. Binding, resistance to the DNase I and SDS-induced release of pcDNA3-EGFP from vectors

The capacity to bind, protect and release the plasmid pcDNA3-EGFP from BE2-SLN_1 and BE3-SLN_1 vectors (Figure 2A), as well as from SLN_2-based complexes (Figure 2B) was evaluated using agarose gel electrophoresis. DX-SLN_1 and HA-SLN_1 have been shown to adequately bind, protect and release DNA in previous studies [20, 22].

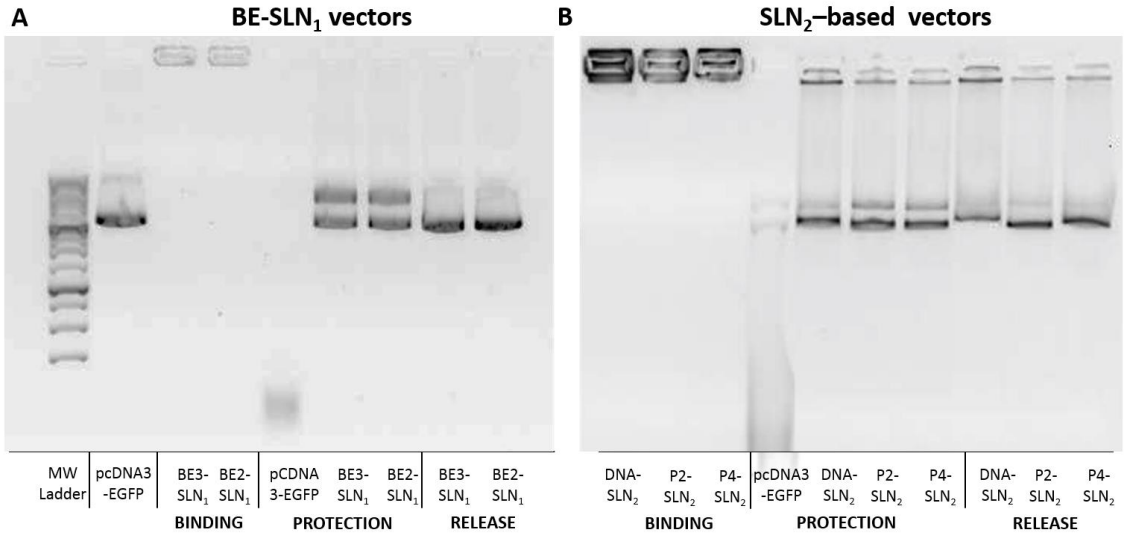

Fig.2. Binding, protection and release of pcDNA3-EGFP from BE-SLN_1 vectors (A) and SLN_2-based vectors. MW ladder corresponds to the 1 kb DNA ladder from NIPPON Genetics Europe.

In the binding studies, the vectors were placed in the wells at a final concentration of 0.03 μg DNA/μl, and the absence of bands in the corresponding lanes demonstrated that DNA was fully bound to the vectors in all cases.

The capacity of the vectors to release the plasmid was studied treating the vectors with SDS for 5 min, prior to placement in the wells. SDS is able to break the interaction between SLNs and DNA without disruption of the structure of lipid nanoparticles. Nevertheless, when the plasmid is too highly condensed by SLNs the release does not occur. After the SDS treatment of the SLN_1-based vectors, DNA was able to migrate from the loading wells, which demonstrates its ability to be completely released. However, the plasmid was partially detected in the loading wells that correspond to the SLN_2-based vectors (lanes 8-10), which indicates that complete release was not achieved.

In order to evaluate the protection capacity, before addition of the vectors to the gel, they were first incubated with DNase I for 30 min, and later SDS was added to the mixture. All formulations were able to protect the plasmid, while free DNA was totally degraded (lane 5 in gel A, and lane 4 in gel B). After treatment with DNase I the plasmid released from the formulations showed two bands, while the control plasmid (lane 2 in figure 2A) only showed one band. The lower band (which shows high intensity) corresponds to the supercoiled form (SC) and the upper band to the open circular form (OC). The change detected in the bands indicates that DNase I turned the SC form, which is the DNA topology with the most transfection capacity, into OC by cutting one of the DNA double strands.

3.4. GFP transfection and cell viability in vitro

Transfection efficacy of pcDNA3-EGFP bearing vectors was determined 72 hours after treatment with the vectors. The percentage of HCE-2 transfected cells and the amount of GFP, that was expressed as RFUs, were measured. Cell viability was also evaluated at that time. In the case of the SLN_2-based vectors, only the results of the vector P4-SLN_2 are represented, as the other vectors were not able to transfect. The transfection efficacy and cell viability of the BE2-SLN_1 and BE3-SLN_1 vectors were similar, and the former was used in the following studies. The naked plasmid and the complexes without SLNs were also added to the cells in the same conditions, resulting in no transfection.

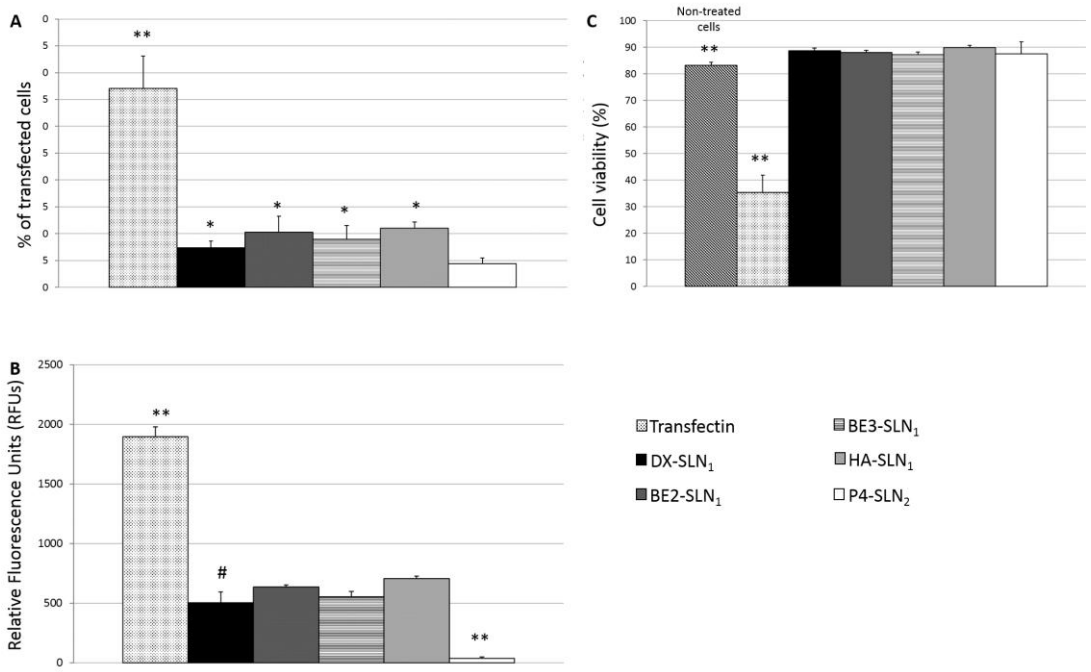

*Fig.3. (A) Percentage of transfected HCE-2 cells 72 hours after treatment with the pcDNA3-EGFP vectors. (B) Relative fluorescence units (RFUs) of transfected HCE-2 cells 72h after treatment with the pcDNA3-EGFP vectors. (C) Cell viability 72 hours after the treatment of HCE2 cells with the pcDNA3-EGFP vectors. (n=3; data are expressed as mean ± standard deviation). ** $p<0.01$ with respect to the other formulations; * $p<0.05$ with respect to P4-SLN_2; # $p<0.05$ with respect to BE2-SLN_1 and HA-SLN_1.*

The SLN_2-based vectors were found to be less effective than the SLN_1-based vectors in terms of the percentage of transfected cells ($p<0.05$) and RFUs ($p<0.01$). While commercial TransFectin was found to be more effective than SLN-based vectors ($p<0.01$), cell viability (Figure 3C) decreased drastically (35% of viable cells). Cell viability, after the treatment of HCE-2 cells with the SLN-based vectors, was over 85%, and did not show differences compared to the non-treated cells and to the cells treated with the naked plasmid and the complexes without SLNs (data not shown).

3.5. Uptake of Nile Red-labelled SLNs in HCE-2 cells

Nile Red-labeled vectors were added to HCE-2 culture cells, and after 2 hours of incubation cells were washed with PBS and detached from the wells. Vector entry into the cells was analysed using flow cytometry; the results are represented in the histograms in Figure 4. The displacement to the right of the histograms that correspond to the cells treated with the vectors, compared to the histogram that belongs to the non-treated cells (filled grey), indicates that Nile Red-labelled vectors entered all the cells in

all cases. The variations in the displacements describe the different fluorescence intensities in the cells (expressed as the X mean in the graph). Those changes are related to the SLN to plasmid ratios; 2 to 1 in HA-SLN_1, which showed less intensity, 5 to 1 in DX-SLN_1 and BE-SLN_1, which were in the middle, and 10 to 1 in the P4-SLN_2 vectors, which gave the highest intensity.

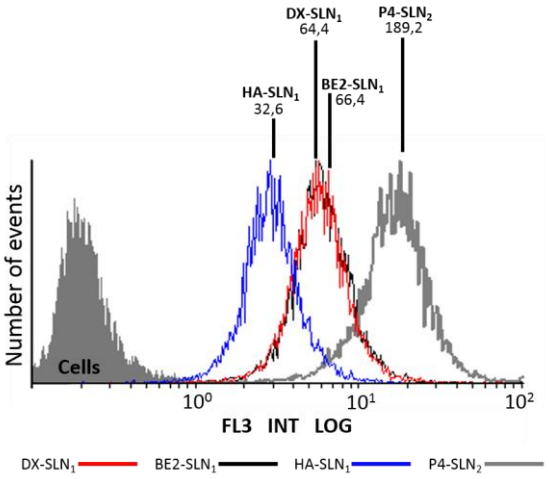

Fig.4. Flow cytometry analysis of cellular uptake of vectors, using Nile Red-labelled SLNs in HCE-2 cells. The values indicated over the lines correspond to the X mean intensity of fluorescence.

3.6. Intracellular disposition

In order to study vector distribution into HCE-2 cells, DX-SLN_1, BE2-SLN_1, HA-SLN_1 and P4-SLN_2 vectors containing the plasmid labelled with EMA (red fluorescence) were added to the culture cells, and at different times (4, 12 and 24 hours), cells were washed, fixed and mounted with DAPI-fluoromount-G™, to label nuclei in blue. Figure 5 shows the images acquired by inverted fluorescence, where differences in terms of intracellular DNA condensation and distribution were observed. When the plasmid is highly condensed, due to the electrostatic interactions with the components of the vectors, red fluorescence appears dotted (arrow heads). Along the time, and due to the interaction of the vectors with intracellular components, plasmid de-condensation occurs, which results in a more diffused fluorescence (asterisks).

In the case of the BE2-SLN_1 and DX-SLN_1 vectors, the plasmid appeared condensed 4 hours after transfection, but at 12 and 24 hours, the diffused red fluorescence indicates plasmid de-condensation. The plasmid in the P4-SLN_2 vectors remained highly condensed even 24 hours after the treatment of the cells, while DNA in the HA-SLN_1

vectors was seen to be poorly condensed in the cytoplasm from 4 hours post-transfection.

Regarding the intracellular disposition, the plasmid appeared to be dispersed all over the cytoplasm and in the perinuclear area at 4 hours, while, after 12 hours, the plasmid was also located in the nucleus of some cells, which is necessary for gene expression. However, in the case of the P4-SLN_2 vectors the plasmid was hardly detected in the nuclei.

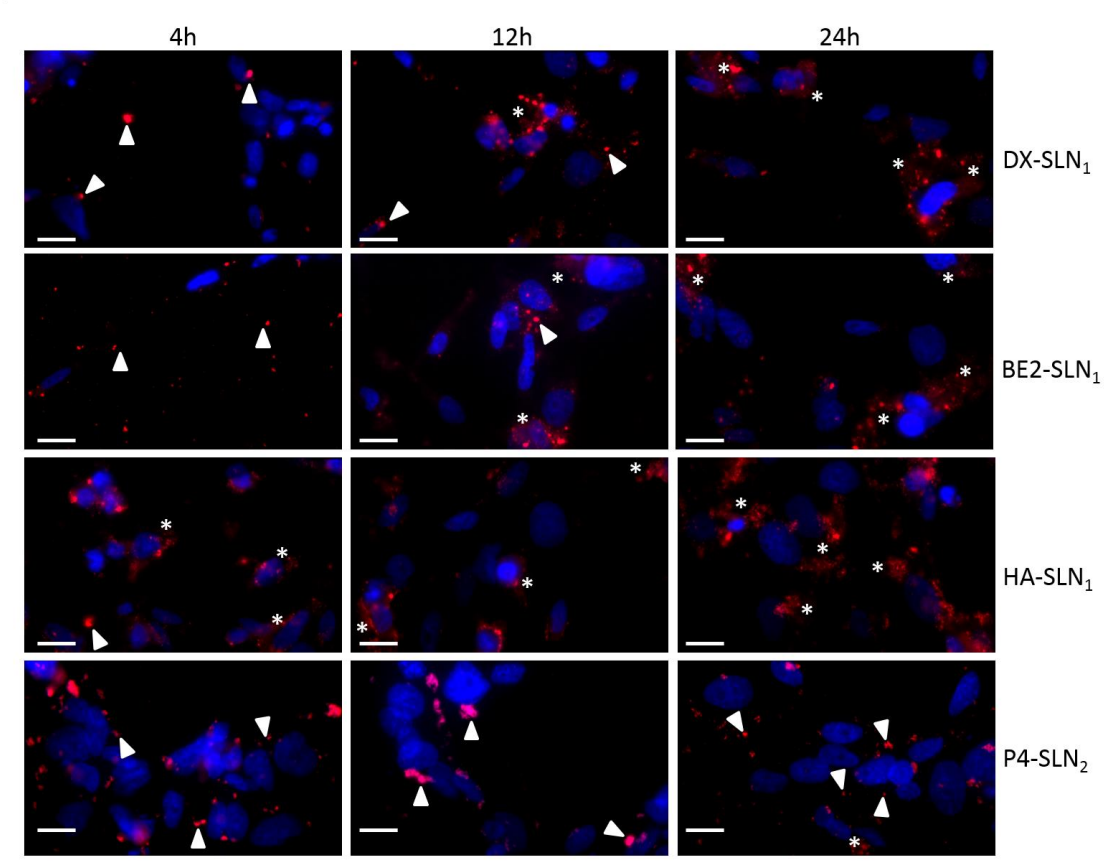

Fig.5. Fluorescence microscopy images 4, 12 and 24 hours after the addition of vectors containing the EMA-labelled plasmid (red) in HCE-2 cells. Nuclei were labelled with DAPI (blue). Arrow heads indicate areas where condensed plasmid was detected; asterisks indicate areas where de-condensed plasmid was detected. Magnification 60X. Scale bar: 20 µm.

3.7. Ex vivo studies

3.7.1. Internalization in cornea explants

Internalization in cornea tissue was qualitatively analysed using fluorescence microscopy with Nile Red-labelled SLNs. In optical microscopy endothelial layer can be observed clearly, after addition of Alizarin Red dye to the endothelial side, in order to increase the contrast of cell margins for observation in normal light mode. Since the

dye can interfere in the fluorescence study, alternative nuclei staining was obtained with DAPI, added to the endothelial side, and only fluorescence images are provided. Two hours after incubation with Nile Red-labelled vectors, red fluorescence was detected around the DAPI stained nuclei, while 24 hours later it was co-localized with the DAPI stained nuclei, thus resulting in violet merging of cells. Figure 6 shows a representative distribution of Nile Red-labelled DX-SLN_1 vectors in cornea tissue. Images of untreated corneas were included as reference. Uptake of topically administered nanoparticles is mainly limited by the corneal barriers, among which the epithelial layer; thus, in this preliminary internalization study the demonstrated uptake in the underlying endothelial cells assesses the overcoming of corneal barriers.

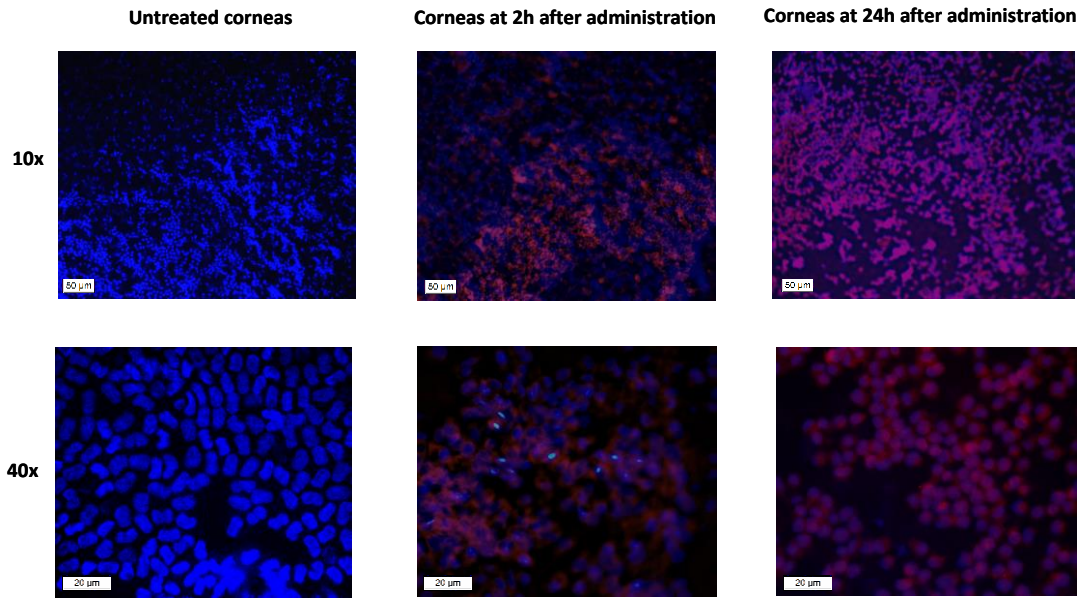

Fig. 6. Fluorescence microscopy images (above: 10x, below: 40x) of Nile Red-labelled DX-SLN_1 internalization in cornea tissue. Left: untreated corneas; middle: two hours after incubation; right: two hours after incubation and 24 hours in Steinhardt medium at 37°C.

3.7.2. Transfection in cornea explants

Figure 7 shows GFP detection by immunofluorescence, 48h after treating cornea tissue with the vectors containing pcDNA3-EGFP plasmid. Three rabbit corneas were treated with each vector, and for protein detection, six cryosections from each eye were immunolabeled and observed using inverted fluorescence microscopy. As control, the immunofluorescence procedure was also carried out in non-treated corneas, and no green fluorescence was detected. Cryosections were obtained from the periphery and from the centre of the cornea. In all the sections obtained from the treated corneas GFP

was detected. However, the distribution of transfected cells differed according to composition of the vectors. DX-SLN_1 induced GFP expression in the epithelium, stroma and endothelium, HA-SLN_1 in the epithelium and stroma, while the BE2-SLN_1 and P4-SLN_2 vectors were only able to transfect epithelial cells.

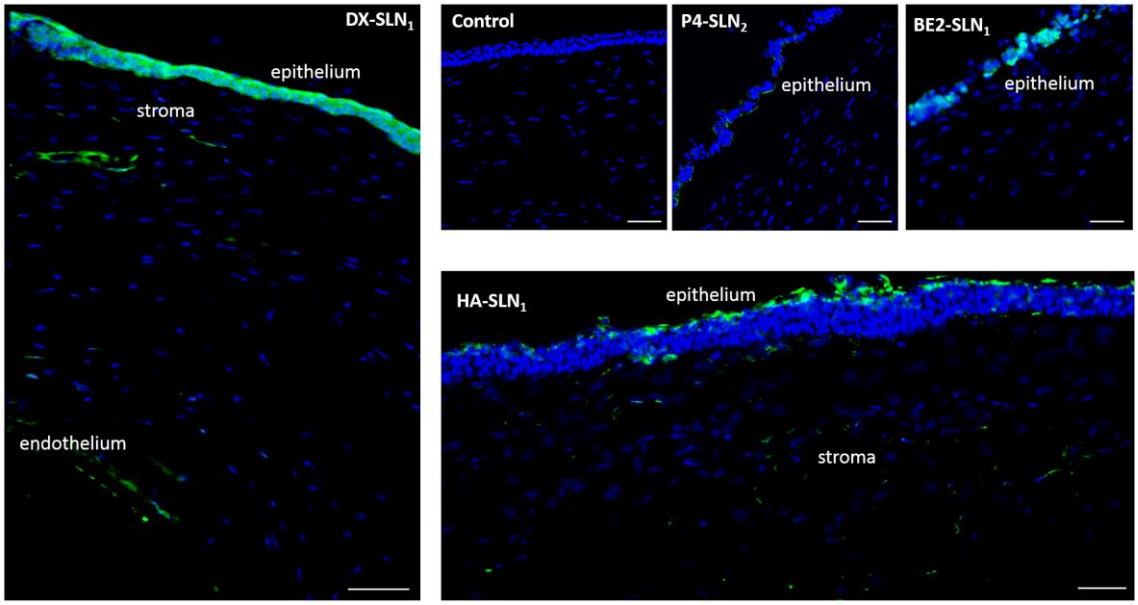

Fig.7. GFP transfection in explanted rabbit corneas 48 hours after treatment with DX-SLN1 (left), BE2-SLN1 (above right), P4-SLN2 (above middle) and HA-SLN1 (bellow). As control (above left) a non-treated cornea immunolabelled with primary and secondary antibodies has been included. Scale bar: 50 µm.

3.7.3. Trichromic study

Masson´s trichrome staining was carried out in six histological sections from each eye, that were obtained from the centre and from the periphery of each cornea. The microscopic images (Figure 8) revealed that no difference was present in the structures of non-treated corneas (Figure 8A) and transfected tissues. Both treated and non-treated corneas were kept in Steinhardt medium at 37°C for 48 hours in order to compare the effect of the vectors and avoid any interference that may be caused by the cornea handling procedure. The images show that the non-viral SLN-based vectors did not alter the corneal structure, since the treated corneas (B, C, D, E) showed an architecture close to the non-treated rabbit corneas (A).

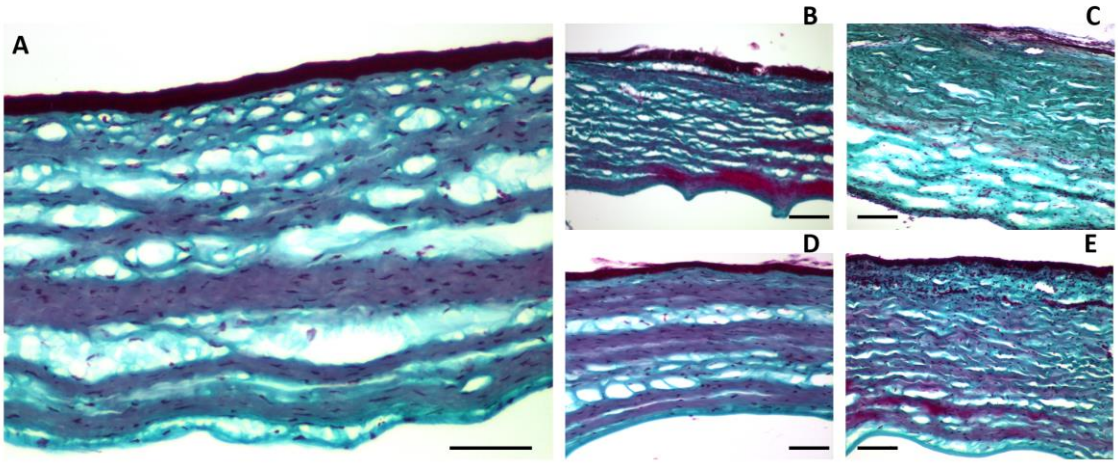

Fig.8. Microscope image of cornea tissues stained using Masson´s trichrome technique. A: non-treated cornea; B: cornea treated with DX-SLN$_1$; C: cornea treated with BE2-SLN$_1$; D: cornea treated with HA-SLN$_1$; E: cornea treated with P4-SLN$_2$. Scale bar: 50 µm.

3.8. Studies with pUNO1-hIL10

3.8.1. Vector characterization

Differences in the plasmid size may affect the final features of the SLN-based vectors. Therefore, the delivery systems containing pUNO1-hIL10 were also characterized in terms of size, PDI and zeta potential (Table 5). The vector P4-SLN$_2$ had a larger size (510.7 nm) than the SLN$_1$-based vectors. Surface charge was positive, at around +36 mV, in the case of BE2-SLN$_1$ and DX-SLN$_1$, and lower in the case of HA-SLN$_1$ and P4-SLN$_2$, at around +29 mV. PDI was under 0.45 in all cases and did not show statistical differences.

Table 5. Physicochemical characterization of SLN-based vectors bearing the plasmid pUNO1-hIL10. PDI (Polydispersity index). (n=3; data are expressed as mean ± standard deviation).

Vectors with pUNO1-hIL10	Size (nm)	PDI	Zeta potential (mV)
DX-SLN$_1$	233.1 ± 81.7	0.36 ± 0.10	+36.1 ± 2.2
BE2-SLN$_1$	290.1 ± 20.8	0.34 ± 0.03	+36.6 ± 4.6
HA-SLN$_1$	242.1 ± 38.0	0.35 ± 0.04	+29.6 ± 0.8$^{\#}$
P4-SLN$_2$	510.7 ± 81.2*	0.44 ± 0.03	+29.5 ± 2.2$^{\#}$

**p<0.05 with respect to the other formulations. #p<0.05 with respect to BE2-SLN$_1$ and DX-SLN$_1$.*

3.8.2. Agarose gel electrophoresis

The binding, protection and release capacity of the vectors are also influenced by the size of the plasmid. Figure 9 shows the gel electrophoresis for the study of these characteristics in the vectors that bare the plasmid pUNO1-hIL10, that was performed as previously explained for pcDNA3-GFP vectors.

SLN_1-based vectors were able to bind, protect and release the plasmid properly. However, in the case of SLN_2-based vectors, the plasmid hardly migrated through the gel (lanes 11 and 15), which indicates that it was scarcely released from the vectors.

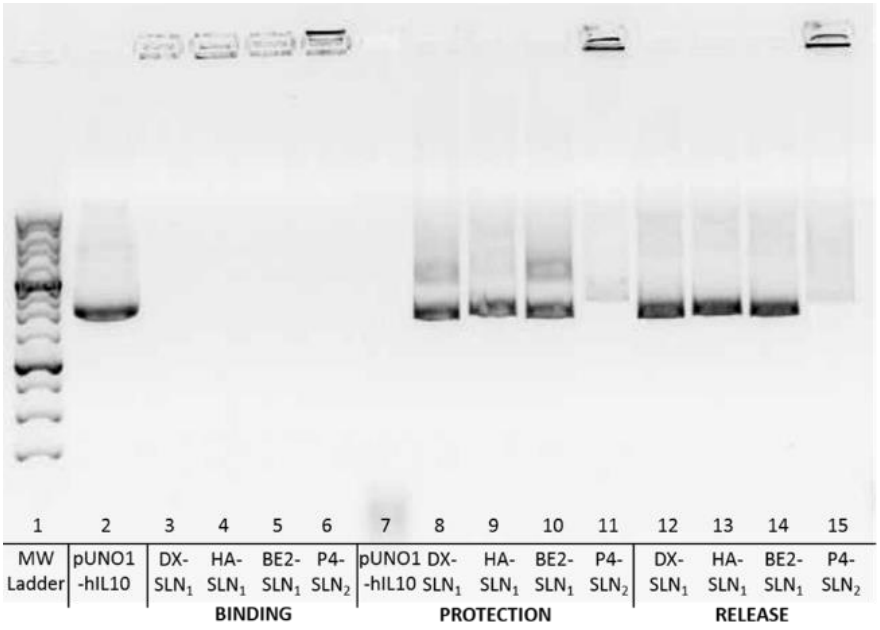

Fig.9. Study of the binding, protection and release of the vectors formed with pUNO1-hIL10. Protection samples were treated with DNase I and SDS, and samples of release lanes, only with SDS. MW ladder corresponds to the 1 kb DNA ladder from NIPPON Genetics Europe.

3.8.3. Transfection efficacy with pUNO1-hIL10

IL-10 levels secreted by HCE-2 cells 72 hours after treatment with the vectors were analysed by ELISA in the culture medium of the cells. The basal production of non-treated cells was not detectable. In addition, in order to analyse the effect of the SLNs in the IL-10 production by HCE-2 cells, vectors bearing the plasmid pcDNA3-EGFP instead of pUNO1-hIL10 were used for transfection, and IL-10 levels were also undetectable. SLN-based vectors induced IL-10 expression and, as can be seen in figure 10, transfection with SLN_1-based vectors resulted in higher extracellular IL-10 levels (over 10,000 pg/mL) than were caused by SLN_2-based vectors (100 pg/mL). Intracellular levels of the cytokine were under 200 pg/mL in all cases.

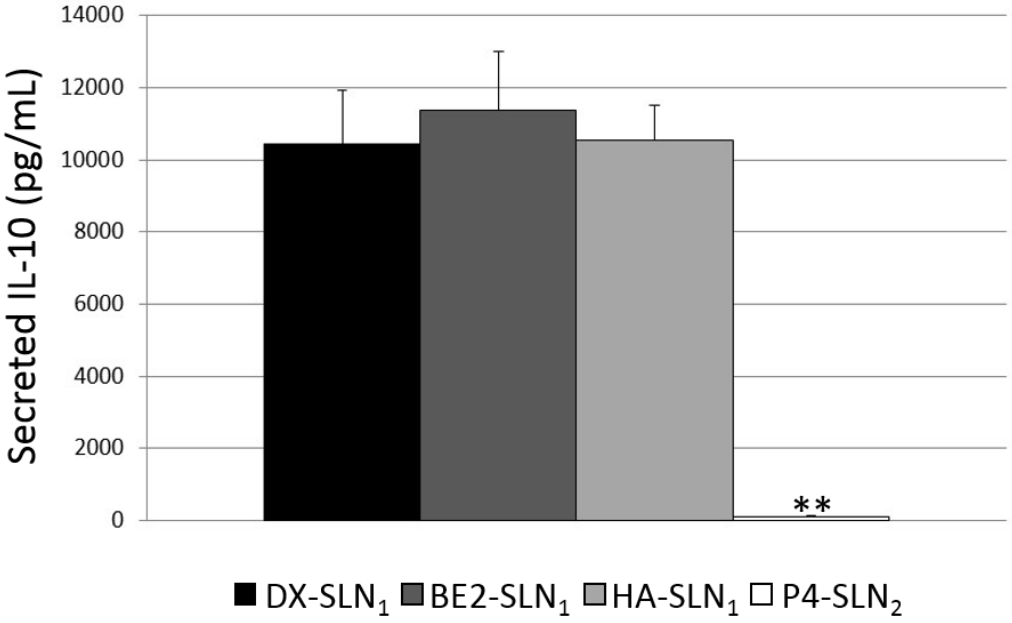

*Fig. 10. Levels of IL-10 secreted by HCE-2 cells 72h after treatment with SLN-based vectors bearing the plasmid pUNO1-hIL10. **p<0.01 with respect to the other formulations.*

4. Discussion

Gene therapy is a promising treatment for corneal inflammation, as it is a strategy to delivery potent anti-inflammatory genes, such as the one that encodes IL-10, in order to induce a long-term anti-inflammatory response through the *de novo* synthesis of cytokines. Additionally, the fact that it can be administered topically on the corneal surface, and over repeated administrations, makes this therapeutic approach very advantageous. However, limitations to the capacity of delivery systems to overcome the physiological obstacles to transfection, such as precorneal (tear turnover, nasolachrymal drainage) and corneal (tight junctions and hydrophobicity of epithelium) barriers, tissue-selective targeting, cell internalization, escape from endo-lysosomal vesicles, movement through the cytoplasm and entry into the nucleus [31], are still partially unresolved.

This work evaluates two types of cationic SLNs, which differ both in preparation method and composition, as non-viral vectors for corneal gene therapy. SLN_1, which have demonstrated a good capacity to act as non-viral vectors, were prepared using the classical solvent-emulsification technique [22], while SLN_2 were prepared by means of the newer solvent-free method, named coacervation [27, 28], as an alternative for comparison. The avoidance of solvents during SLN production is an advantageous

feature of this second type of lipid nanoparticles. SLN_1 showed higher zeta potential than SLN_2, mainly due to the presence of DOTAP, which is more cationic in character than CH, the cationic agent included in SLN_2. It is important to note that the superficial charge of cationic SLNs designed for gene therapy determines DNA condensation capacity, and uperficial charge value of the final complexes [23].

SLNs were electrostatically combined with the peptide protamine and a variety of polysaccharides to form the final complexes with plasmids. The vectors were characterized in terms of size, superficial charge and shape, since these physicochemical properties have significant effects on bio-distribution and cellular internalization [32, 33]. All the vectors presented particle sizes in the nanometre range, making them suitable for retention and corneal permeation after topical administration [14], and positive superficial charge. This cationic surface facilitates the cellular uptake of the nanoparticulate systems [30], thanks to interactions with the negatively charged cell membrane. Furthermore, after topical administration onto the surface of the eye, cationic vectors interact with the negatively charged mucus, thus favouring retention at the corneal surface and improving corneal permeation via endocytic uptake by epithelial cells [16]. In SLN_2-vectors, the proportion of protamine and SLNs with respect to DNA had to be increased (up to protamine:DNA 4:1 and DNA:SLN 1:10) to ensure a cationic surface (at +26 mV). Either the absence of protamine or the use of lower ratios (DNA-SLN2 and P2-SLN2 formulations), resulted in almost neutral vectors in terms of superficial charge, and they were not able to transfect culture cells.

HA-SLN_1 and DX-SLN_1 vectors have previously proven themselves able to transfect a variety of cells *in vitro* and *in vivo* [19, 21, 23], and their capacity to transfect corneal cells both *in vitro* and *ex vivo* has also been demonstrated in this work. One of the other two new vectors designed to transfect the cornea was prepared with BE. This is a second-generation low molecular weight heparin (LMWH) with a mean MW of 3.6 KDa. LMWHs are anticoagulant drugs that also possess anti-inflammatory effects [34], and the BE in the vectors may contribute to this effect. The plasmid in BE2-SLN_1 was adequately condensed, protected and released, due, in part, to the protamine, which is an excellent aid for transfection that is mediated by lipid-based vectors (DNA condenser, it has nuclear localization signals that translocate DNA from the cytoplasm to the nucleus, and it improves transcriptional activity) [24]. This peptide was also used to prepare complexes with SLN_2. TEM images showed that these SLN_2-vectors had a spherical

shape. Previous studies have shown that spherical SLN-based vectors are well taken up by different types of cells [20, 24]. The shape of nanoparticulate systems is important since it influences their cellular internalization; it has been documented that the higher surface area of elongated nanoparticles facilitates their interaction with cell surfaces, and provides higher adhesion to cells compared to spherical nanoparticles [35], whereas the spherical shape favours cellular uptake better than an ellipsoidal shape [36].

In order to test the usefulness of the SLN-based vectors as gene delivery systems for the cornea, transfection studies were carried out in HCE-2 cells with the reporter plasmid pcDNA3-EGFP, and with the therapeutic plasmid pUNO1-IL10, which encodes the anti-inflammatory cytokine IL-10. The levels of this cytokine secreted by HCE-2 cells treated with the most effective formulations were over 1 ng/ml, which are expected to exert an anti-inflammatory effect. In this sense, in a recent work published by Wang et al. [37] IL-10 levels at 0.8 ng/mL in a three-dimensional inflammation model resulted in reduction of pro-inflammatory cytokines, such as TNF-α, and successful inhibition of inflammation. Moreover, the presence of the hybrid promoter EF-1α/HTLV in the plasmid that contains the IL-10 gene, will be likely useful to yield persistent expression of the anti-inflammatory cytokine in vivo [38].

Regardless of the plasmid used, the P4-SLN_2 formulation was found to be less effective than SLN_1-based vectors. Since entry into cells was not a limitation for any of the vectors (Figure 4), the difference in transfection levels may be related to the intracellular behaviour of the formulations. Plasmids must be protected if they are to avoid degradation by intracellular components, but they must also be released in the cytoplasm if they are to enter the nucleus. The intracellular disposition of the DNA (Figure 5), together with the only partial release of the plasmid from SLN_2-based vectors in electrophoresis gel (Figure 2B), indicates that the plasmid was more condensed, even after 24 hours, than was the case with SLN_1-based vectors. The degree of DNA condensation conditions the capacity to bind, release and protect the plasmid, and it depends on the electrostatic interactions with the cationic components of the formulations. CH, the cationic polysaccharide included in SLN_2, binds electrostatically the DNA strongly and efficiently, and protects it from nuclease degradation, but the release of the DNA is compromised. In a previous work [22], in line with these results, non-viral vectors composed of cationic SLNs and oligochitosans, showed a high DNA condensation degree, that resulted in poor transfection of cultured cells *in vitro*.

However, after intravenous administration, transfection was detected in a number of organs. This lack of correlation highlights the necessity to develop models for the evaluation of new delivery systems, at earliest phases of the development process, that better match *in vivo* condictions.

In this sense, cornea explants best mimic *in vivo* behaviour, as the various layers of the cornea are intact. The outermost layer is the epithelium, which is composed of several layers of cells that constantly undergo mitosis. Behind the epithelial cells, there is a transparent film called Bowman's layer, which is composed of collagen. This protein is also the main component of the next layer, the stroma. This is the thickest layer of the cornea and contains fibroblasts (keratocytes), which are plane cells aligned in parallel to the ocular surface and produce the collagen. The layer behind the stroma is Descemet's membrane, which is made up of collagen fibres synthesised by the cells that form the corneal endothelium, the innermost layer. Endothelial cells form a monolayer and are amitotic in humans. Unlike other animal models, such as rodents, corneal endothelial cells in rabbits have limited replicative ability and thus resemble human corneal endothelia [39]. All the vectors were able to transfect corneal tissue (Figure 7) in explants from rabbits, although the distribution of transfected corneal cells varied according to the ligands in the formulations. Vectors formulated with CH and BE were only able to transfect the epithelium, while HA also allowed the transfection of stromal cells to occur. The vector that was prepared with DX was observed to be the most effective, since the green protein was detected abundantly in the epithelium, and also in the stroma and in endothelium. The transfection of the endothelium, formed of non-mitotic cells, is an appropriate target for corneal diseases, as gene expression duration, which is a common limitation of non-viral vectors, can be maintained for longer in cells that do not undergo cell division. The *ex vivo* transfection obtained using DX-SLN_1 vectors matches an *in vivo* study in rats [40], in which GFP expression was detected in the corneal epithelium, stroma and endothelium after topical administration of a similar formulation in the eye. These results confirm that the explanted corneas from rabbits are a good model with which to evaluate new gene therapy-based formulations .

5. Conclusions

SLN-based vectors are promising gene delivery systems for topical administration to the eye, where they can facilitate IL-10 synthesis by corneal cells, making them useful for treating inflammation-related eye surface diseases. Vectors were able to transfect the

epithelium, the stroma, and even the endothelium to varying degrees according to SLN composition and polysaccharide surface coating . SLN-based non-viral vectors could be designed to modulate biodistribution and therefore transfection within the cell layers of the cornea, according to expected therapeutic effect and duration of action.

Summary Points:

- Inflammation is an underlying process in severe ocular surface diseases that result in vision loss and quality-of-life impairment and that currently lacks, effective and safe therapy.
- The topical administration of interleukin-10 (IL-10), a potent anti-inflammatory agent, to treat corneal inflammation is limited by its low bioavailability and short half-life
- Gene supplementation in the cornea, with plasmids that encode for IL10 will lead to the sustained *de novo* synthesis of the cytokine in corneal cells, providing long-term anti-inflammatory effects, although suitable delivery systems are needed for this goal.
- Non-viral vectors that are based on solid lipid nanoparticles (SLNs) can enhance corneal penetration and cellular uptake, extend ocular retention time and provide a controlled release profile, improving ocular bioavailability, and therefore leading to successful corneal gene therapy.
- SLN-based vectors may be functionalized with the aim of modulating the interactions with target cells and improving cellular uptake in order to achieve suitable intracellular distribution for the genetic material as well as its entry into the nucleus.
- SLN-based vectors, which were prepared using different methods and compositions, were able to enter corneal epithelial cells *in vitro* and to induce IL-10 synthesis.
- SLN-based vectors were able to transfect explanted rabbit corneas. The distribution of the transfected corneal cells varied according to their surface decoration.
- Vectors formulated with CH and BE were only able to transfect the corneal epithelium, HA also transfected stromal cells, and the vector prepared with DX also transfected the stroma and even the endothelium.

- SLN-based non-viral vectors could be designed to modulate biodistribution and therefore transfection within the cell layers of the cornea, according to expected therapeutic effect and duration of action.

Figure legends

Figure 1. TEM photographs of (A) SLN_2 and (B) P4-SLN_2 vectors. Scale bar: 200 nm.

Figure 2. Binding, protection and release of pcDNA3-EGFP from BE-SLN_1 vectors (A) and SLN_2-based vectors. MW ladder corresponds to the 1 kb DNA ladder from NIPPON Genetics Europe.

*Figure 3. (A) Percentage of transfected HCE-2 cells 72 hours after treatment with the pcDNA3-EGFP vectors. (B) Relative fluorescence units (RFUs) of transfected HCE-2 cells 72h after treatment with the pcDNA3-EGFP vectors. (C) Cell viability 72 hours after the treatment of HCE2 cells with the pcDNA3-EGFP vectors. (n=3; data are expressed as mean ± standard deviation). ** $p<0.01$ with respect to the other formulations; * $p<0.05$ with respect to P4-SLN_2; # $p<0.05$ with respect to BE2-SLN_1 and HA-SLN_1.*

Figure 4. Flow cytometry analysis of cellular uptake of vectors using Nile Red-labelled SLNs in HCE-2 cells. The values indicated over the lines correspond to the X mean intensity of fluorescence.

Figure 5. Fluorescence microscopy images 4, 12 and 24 hours after the addition of vectors containing the EMA-labelled plasmid (red) in HCE-2 cells. Nuclei were labelled with DAPI (blue). Arrow heads indicate areas where condensed plasmid was detected; asterisks indicate areas where de-condensed plasmid was detected. Magnification 60X. Scale bar: 20 µm.

Figure 6. Fluorescence microscopy images (above: 10x, below: 40x) of Nile Red-labelled DX-SLN_1 internalization in cornea tissue. Left: untreated corneas; middle: two hours after incubation; right: two hours after incubation and 24 hours in Steinhardt medium at 37°C.

Figure 7. GFP transfection in explanted rabbit corneas 48 hours after treatment with DX-SLN1 (left), BE2-SLN1 (above right), P4-SLN2 (above middle) and HA-SLN1 (bellow). As control (above left) a non-treated cornea immunolabelled with primary and secondary antibodies has been included. Scale bar: 50 µm.

Figure 8. Microscope image of cornea tissues stained using Masson´s trichrome technique. A: non-treated cornea; B: cornea treated with DX-SLN1; C: cornea treated with BE2-SLN1; D: cornea treated with HA-SLN1; E: cornea treated with P4-SLN2. Scale bar: 50 µm.

Figure 9. Study of the binding, protection and release of vectors formed with pUNO1-hIL10. Protection samples were treated with DNase I and SDS, and samples of release lanes, only with SDS. MW ladder corresponds to the 1 kb DNA ladder from NIPPON Genetics Europe.

*Figure 10. Levels of IL-10 secreted by HCE-2 cells 72h after treatment with SLN-based vectors bearing the plasmid pUNO1-hIL10. **p<0.01 with respect to the other formulations.*

Table Legends

Table 1. Weight ratios of the vectors prepared and evaluated.

Table 2. Physicochemical characterization of SLN1 and SLN2. PDI (Polydispersity index). (n=3; data are expressed as mean ± standard deviation).

Table 3. Physicochemical characterization of SLN1-based vectors bearing the plasmid pcDNA3-EGFP. PDI (Polydispersity index). (n=3; data are expressed as mean ± standard deviation).

Table 4. Physicochemical characterization of SLN2-based vectors bearing the plasmid pcDNA3-EGFP. PDI (Polydispersity index). (n=3; data are expressed as mean ± standard deviation).

Table 5. Physicochemical characterization of SLN-based vectors bearing the plasmid pUNO1-hIL10. PDI (Polydispersity index). (n=3; data are expressed as mean ± standard deviation).

References

[1] Ahsan SM, Rao CM. Condition responsive nanoparticles for managing infection and inflammation in keratitis. *Nanoscale*. 9(28), 9946-9959 (2017).

[2] Soriano-Romaní L, Vicario-de-la-Torre M, Crespo-Moral M, López-García A, Herrero-Vanrell R, Molina-Martínez IT *et al*. Novel anti-inflammatory liposomal formulation for the pre-ocular tear film: In vitro and ex vivo functionality studies in corneal epithelial cells. *Exp Eye Res*. 154, 79-87 (2017).

[3] Calles JA, López-García A, Vallés EM, Palma SD, Diebold Y. Preliminary characterization of dexamethasone-loaded cross-linked hyaluronic acid films for topical ocular therapy. *Int J Pharm*. 509(1-2), 237-243 (2016).

[4] Saxena A, Khosraviani S, Noel S, Mohan D, Donner T, Hamad AR. Interleukin-10 paradox: A potent immunoregulatory cytokine that has been difficult to harness for immunotherapy. *Cytokine*. 74(1), 27-34 (2015).

[5] Engelhardt KR, Grimbacher B. IL-10 in humans: lessons from the gut, IL-10/IL-10 receptor deficiencies, and IL-10 polymorphisms. *Curr Top Microbiol Immunol*. 380, 1-18 (2014).

[6] Lobo-Silva D, Carriche GM, Castro AG, Roque S, Saraiva M. Balancing the immune response in the brain: IL-10 and its regulation. *J Neuroinflammation*. 13(1), 297 (2016).

[7] Machuca TN, Cypel M, Bonato R, Yeung JC, Chun YM, Juvet S *et al*. Safety and efficacy of ex vivo donor lung adenoviral IL-10 gene therapy in a large animal lung transplant survival model. *Hum Gene Ther*. 28(9), 757-765 (2017).

[8] Kaufmann C, Mortimer LA, Brereton HM, Irani YD, Parker DG, Anson DS *et al*. Interleukin-10 gene transfer in rat limbal transplantation. *Curr Eye Res*. 42(11), 1426-1434 (2017).

[9] Tahvildari M, Emami-Naeini P, Omoto M, Mashaghi A, Chauhan SK, Dana R. Treatment of donor corneal tissue with immunomodulatory cytokines: a novel strategy to promote graft survival in high-risk corneal transplantation. *Sci Rep*. 7, 971 (2017).

[0] Azher TN, Yin XT, Stuart PM. Understanding the role of chemokines and cytokines in experimental models of herpes simplex keratitis. *J Immunol Res*. 2017, 7261980 (2017). *This work reviews the protective role of IL-10 in Herpes simplex keratitis and proposes this molecule as a possible target of future therapy

[1] Mohan RR, Rodier JT, Sharma A. (2013) Corneal gene therapy: basic science and translational perspective. *The Ocular Surface*. 11 (3), 150–164 (2013).

[2] Solinís MÁ, del Pozo-Rodríguez A, Apaolaza PS, Rodríguez-Gascón A. Treatment of ocular disorders by gene therapy. *Eur J Pharm Biopharm*. 95(Pt B), 331-342 (2015).

[3] Sengel-Turk CT, Gumustas M, Uslu B, Ozkan S.A. Nanosized Drug Carriers for Oral Delivery of Anticancer Compounds and the Importance of the Chromatographic Techniques. In: *Nano- and Microscale Drug Delivery Systems*, Grumezescu AM (Ed.), Elsevier, Amsterdam, Netherlands, 165–195 (2017).

[4] Seyfoddin A, Al-Kassas R. Development of solid lipid nanoparticles and nanostructured lipid carriers for improving ocular delivery of acyclovir. *Drug Dev Ind Pharm*. 39(4), 508-519 (2013).

[15] Battaglia L, Serpe L, Foglietta F, Muntoni E, Gallarate M, del Pozo-Rodríguez A *et al*. Application of lipid nanoparticles to ocular drug delivery. *Expert Opin Drug Deliv*. 13(12), 1743-1757 (2016).

[6] Bachu RD, Chowdhury P, Al-Saedi ZHF, Karla PK, Boddu SHS. Ocular Drug Delivery Barriers-Role of Nanocarriers in the Treatment of Anterior Segment Ocular Diseases. *Pharmaceutics*. 10(1) pii: E28 (2018). ** This is a recent review about the main ocular barriers to anterior segment ocular delivery, and the nanocarrier systems designed to overcome these barriers. Among those systems the advantages of SLNs are described.

[7] Maiti S, Jana S. Biocomposites in ocular drug delivery. In: *Biopolymer-Based Composites*. *Drug Delivery and Biomedical Applications*. Jana S, Maiti S, Jana S (Ed.), Elsevier, Amsterdam, Netherlands, 139–168 (2017).

[8] Torrecilla J, del Pozo-Rodríguez A, Apaolaza PS, Solinís MÁ, Rodríguez-Gascón A. Solid lipid nanoparticles as non-viral vector for the treatment of chronic hepatitis C by RNA interference. *Int J Pharm*. 479(1), 181-188 (2015).

[9] Ruiz de Garibay AP, Solinís MA, del Pozo-Rodríguez A, Apaolaza PS, Shen JS, Rodríguez-Gascón A. Solid lipid nanoparticles as non-viral vectors for gene transfection in a cell model of Fabry disease. *J Biomed Nanotechnol*. 11(3), 500-511 (2015).

[20] Torrecilla J, del Pozo-Rodríguez A, Solinís MÁ, Apaolaza PS, Berzal-Herranz B, Romero-López C *et al*. Silencing of hepatitis C virus replication by a non-viral vector based on solid lipid nanoparticles containing a shRNA targeted to the internal ribosome entry site (IRES). *Colloids Surf B Biointerfaces*. 146, 808-817 (2016).

[21] Apaolaza PS, del Pozo-Rodríguez A, Solinís MA, Rodríguez JM, Friedrich U, Torrecilla J *et al*. Structural recovery of the retina in a retinoschisin-deficient mouse after gene replacement therapy by solid lipid nanoparticles. *Biomaterials*. 90, 40-49 (2016).

[22] Delgado D, del Pozo-Rodríguez A, Angeles Solinís M, Bartkowiak A, Rodríguez-Gascón A. New gene delivery system based on oligochitosan and solid lipid nanoparticles: 'in vitro' and 'in vivo' evaluation. *Eur J Pharm Sci*. 50(3-4), 484-491 (2013).

[23] Apaolaza PS, Delgado D, del Pozo-Rodríguez A, Gascón AR, Solinís MÁ. A novel gene therapy vector based on hyaluronic acid and solid lipid nanoparticles for ocular diseases. *Int J Pharm*. 465(1-2), 413-426 (2014).

[24] Apaolaza PS, del Pozo-Rodríguez A, Torrecilla J, Rodríguez-Gascón A, Rodríguez JM, Friedrich U *et al*. Solid lipid nanoparticle-based vectors intended for the treatment of X-linked juvenile retinoschisis by gene therapy: In vivo approaches in Rs1h-deficient mouse model. *J Control Release*. 217, 273-283 (2015). *This work includes the optimization and characterization of HA-SLN_1 vectors for ocular administration.

[25] Chaiyasan W, Srinivas SP, Tiyaboonchai W. Crosslinked chitosan-dextran sulfate nanoparticle for improved topical ocular drug delivery. *Mol Vis*. 21, 1224–1234 (2015).

[26] Widjaja LK, Bora M, Chan PN, Lipik V, Wong TT, Venkatraman SS. Hyaluronic acid-based nanocomposite hydrogels for ocular drug delivery applications. *J Biomed Mater Res A*. 102(9), 3056-3065 (2014).

[27] Chirio D, Gallarate M, Peira E, Battaglia L, Muntoni E, Riganti C *et al*. Positive-charged solid lipid nanoparticles as paclitaxel drug delivery system in glioblastoma treatment. *Eur J Pharm Biopharm*. 88(3), 746-758 (2014). *This work describes the coacervation method used as basis of the preparation technique used to obtain SLN_2

[28] Clemente N, Ferrara B, Gigliotti CL, Boggio E, Capucchio MT, Biasibetti E *et al*. Solid lipid nanoparticles carrying temozolomide for melanoma treatment. Preliminary in Vitro and in vivo studies. *Int J Mol Sci*. 19(2), pii: E255 (2018).

[29] Steinhard RA. Cornea preservation medium. US7087369 B2 (2006).

[30] Battaglia L, D'Addino I, Peira E, Trotta M, Gallarate M. Solid lipid nanoparticles prepared by coacervation method as vehicles for ocular cyclosporine. *J Drug Del Sci Technol*. 22 (2), 125-130 (2012).

[31] Rodríguez-Gascón A, del Pozo-Rodríguez A, Isla A and Solinís, MA. Gene Therapy in the Cornea. In: *eLS.* John Wiley & Sons Ltd, Chichester, UK. (2016).

[32] Salatin S, Maleki Dizaj S, Yari Khosroushahi A. Effect of the surface modification, size, and shape on cellular uptake of nanoparticles. Cell Biol Int. 39(8), 881-890 (2015). ** This works relates the physicochemical characteristics of nanoparticles (size, shape, and the surface modification) to their cellular interaction and uptake into the cells.

[33] Shang L, Nienhaus K, Nienhaus GU. Engineered nanoparticles interacting with cells: size matters. *J Nanobiotechnology*. 12, 5 (2014).

[34] Mastrolia SA, Mazor M, Holcberg G, Leron E, Beharier O, Loverro G *et al*. The physiologic anticoagulant and anti-inflammatory role of heparins and their utility in the prevention of pregnancy complications. *Thromb Haemost*. 113(6), 1236-1246 (2015).

[35] Agarwal R, Singh V, Jurney P, Shi L, Sreenivasan S, Roy K. Mammalian cells preferentially internalize hydrogel nanodiscs over nanorods and use shape-specific uptake mechanisms. *Proc Natl Acad Sci* 110, 17247–17252 (2013).

[36] Dasgupta S, Auth T, Gompper G. Shape and orientation matter for the cellular uptake of nonspherical particles. *Nano Lett* 14, 687–693 (2014).

[37] Wang X, Coradin T, Hélary C. Modulating inflammation in a cutaneous chronic wound model by IL-10 released from collagen-silica nanocomposites via gene delivery. *Biomater Sci* 6, 398-406 (2018).

[38] Sakaguchi M, Watanabe M, Kinoshita R, Kaku H, Ueki H, Futami J, et al. Dramatic increase in expression of a transgene by insertion of promoters downstream of the cargo gene. *Mol Biotechnol* 56, 621-630 (2014).

[39] Zavala J, López Jaime GR, Rodríguez Barrientos CA, Valdez-Garcia J. Corneal endothelium: developmental strategies for regeneration. *Eye (Lond).* 27(5), 579–588 (2013).

[40] Delgado D, del Pozo-Rodríguez A, Solinís MÁ, Avilés-Triqueros M, Weber BH, Fernández E *et al*. Dextran and protamine-based solid lipid nanoparticles as potential vectors for the treatment of X-linked juvenile retinoschisis. *Hum Gene Ther*. 23(4), 345-355 (2012). *This work includes the optimization and characterization of DX-SLN_1 vectors for ocular administration.

*** of interest**

**** of considerable interest**